Appl. Phys. A 67, 107–111 (1998)

Applied Physics A
Materials
Science & Processing

Formation of small single-layer and nested BN cages under electron irradiation of nanotubes and bulk material

O. Stéphan[1,4], Y. Bando[1], A. Loiseau[2], F. Willaime[3], N. Shramchenko[2], T. Tamiya[1], T. Sato[1]

[1] National Institute for Research in Inorganic Materials, Namiki 1–1, Tsukuba, Ibaraki 305, Japan
[2] Laboratoire d'Etudes des Microstructures, UMR n°104, ONERA, 92322 Châtillon, France
[3] Section de Recherches de Métallurgie Physique, Centre d' Etudes de Saclay, 91191 Gif Sur Yvette, France
[4] Laboratoire de Physique des Solides, Université Paris-Sud, 91405 Orsay, France

Received: 2 March 1998

Abstract. An experimental evidence for the formation of small BN cage-like molecules, under electron-irradiation experiments of BN samples, is presented. Depending on the starting material, either close-packed agglomerates of small "fullerenes", or small nested "fullerenes" with up to six layers are found as irradiation derivatives. The overall polyhedral shape of the BN cages is explained within the frame of the octahedral model previously proposed for BN analogs to fullerenes. The diameters of the smallest and most observed cages range from 0.4 to 0.7 nm, and are close to those of the $B_{12}N_{12}$, $B_{16}N_{16}$ and $B_{28}N_{28}$ octahedra which were predicted to be magic clusters for the BN system from electronic structure calculations.

The discovery of the C_{60} soccer ball [1] followed by that of larger fullerenes and carbon nanotubes [2] raised the curtain on a new class of nano-objects based on layered materials with predicted unique physical properties. Recently, the synthesis of BN [3–6], BCN [7, 8], and MoS_2 [9] nanotubes and closed shell nanoparticles has generalized the idea already admitted for carbon that for a small assembly of atoms the network bends and curls into a close structure in order to eliminate the highly unfavorable dangling bonds. Nested concentric BN polyhedra have been successfully synthesized by reaction of BCl_3 with NH_3 in a laser beam [10, 11]. However, in spite of theoretical predictions for the stability of the hybrid $B_{24}C_{12}N_{24}$ molecule [12] and the $B_{12}N_{12}$, $B_{16}N_{16}$, $B_{28}N_{28}$ molecules [13, 14], there has been, so far, no experimental evidence for the stability of structures analogous to C_{60} and other small carbon fullerenes in layered materials other than graphite.

Strong irradiation in an electron microscope allows structural fluidity and a rearrangement of the structure caused by the momentum transfer of high-energy electrons to the nuclei (knock-on collisions). It is now well known that carbon material, whatever its initial structural state – namely amorphous, turbostratic or well-graphitized, bulk crystallites, nanocages, or nanotubes – can be transformed into onion-like structures when submitted to such intense electron irradiation [15, 16]. Carbon onions can have very different sizes and consist of concentric polyhedral fullerene cages; single- or double-layer small fullerene cages can also be formed [17]. On the other hand, only disordered spherical layered structures with incompletely closed layers were shown to form under electron irradiation of crystalline BN [18], MoS_2 crystals [19], and turbostratic BC_2N [20]. We present transformations obtained when submitting to intense irradiation regimes two kinds of BN samples, a turbostratic BN sample and a BN nanotube powder. Depending on the starting material, two different irradiation products are observed: small nested polyhedra or close-packed arrangements of small single-layer cage-like clusters. The size and shape of the smallest observed cage is compared to that of the smallest high-symmetry polyhedral clusters predicted to have particularly high stability [14, 21]. The discrepancy, in particular for the outermost shells, is discussed in terms of possible defects in the ideal structure of the model, made of only six four-member rings and hexagons.

1 Experimental

In the experiments described here, two starting materials were used: a novel turbostratic BN sample with a well-defined interlayer spacing (β-tBN) [22, 23]; and a BN nanotube sample produced by arc discharge between HfB_2 electrodes in a nitrogen atmosphere [5]. Observations were carried out respectively in a field emission 300 kV analytical microscope (Jeol 3000F) and in a Jeol 4000FX (LaB_6 emission filament) transmission electron microscope. The in situ irradiation of the BN samples was made using electron doses up to 10–20 times higher than under normal imaging conditions.

2 Results

2.1 Turbostratic BN *irradiation experiments*

Figure 1 shows a typical sequence of high resolution electron microscopy (HREM) images taken at successive time intervals during intense irradiation with a Jeol 3000F in the

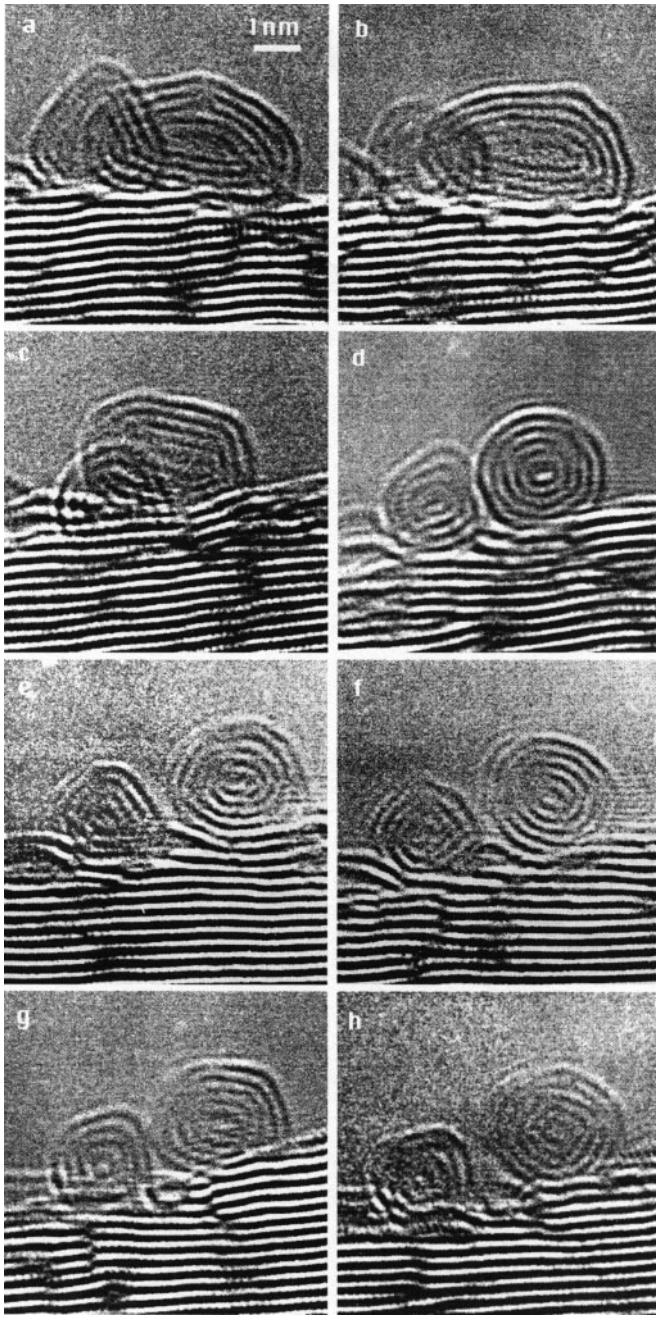

Fig. 1a–h. Temporal sequence showing the in situ formation of two small nested cage-like clusters under strong irradiation of turbostratic BN. **a** Formation of two spirals from the scrolling of the surface plane after ≈ 20 s of strong irradiation. **b** ≈ 40 s. **c** ≈ 80 s. **d** ≈ 100 s. **e** ≈ 120 s. **f** ≈ 140 s. **g** ≈ 160 s. **h** ≈ 200 s. Note the hexagonal-like shape of the small onion 2-D image (labeled I in text) in **e** and the square-like shape of both onion 2-D images in their final configurations (**g** and **h**)

illumination geometry where b-tBN basal planes are parallel to the electron beam. In the initial stage (not shown in Fig. 1), some covalent bonds are broken locally within the surface layer under electron bombardment. Strips of the surface layer – weakly bound with adjacent layer by van der Waals forces – pull off and scroll into spirals. This phenomenon is attributed to electron charge accumulation on the surface. Figure 1a shows the simultaneous formation of two spirals made of 4 and 5 revolutions respectively. The spatial extension of these objects in the direction perpendicular to the image plane as well as their three-dimensional shape are difficult to determine by their 2-D-like projection in the transmission electron micrograph. The overlapping of the fringes, and the very similar and weak interference contrast in both objects, suggest that their dimension in the perpendicular direction is comparable to that along the surface in the image plane, i.e. a few nm. An open-ended rolled carpet shape can be envisaged but the particles are most likely capped also in the perpendicular direction. After 20 s of further irradiation (Fig. 1b), both spirals have closed into a coaxial set of four and five shells respectively. Let us call these objects I and II. The next sequence of images shows the induced fluidity structural transformation of both unstable objects up to a final and stable configuration (Figs. 1g and 1h). This transformation occurs by a decrease of the internal hollow (clearly seen in Fig. 1d). At this stage the structure is believed to have completely evolved towards nested 3-D closed cages in order to eliminate the energetically highly unfavorable dangling bonds.

Thanks to its initial smaller cavity, and its lower number of layers, particle I reaches its stable configuration before particle II (for $140\text{ s} < t < 160$ s, see Fig. 1e). Figure 1d shows an intermediate configuration of particle II where both internal shells are closed and faceted whereas some defects still exist in the stacking of the three outer shells. In Fig. 1g such defects have disappeared though the section is still elongated in shape. One notes as well a shrinkage of the cage under electron irradiation. No shrinkage is observed in Fig. 1h where a stable form is attained.

In their final configurations, the architecture of particles I and II results in the nesting of cages whose 2-D HREM images are square-like in shape. The square-like shape is all the more pronounced as the cages decrease in size. The sides of the innermost squares in onions I and II are 0.48 nm and 0.67 nm respectively. We mention that this overall square-like shape was previously observed in large nested BN polyhedra [11]. The interlayer distance between cages is not constant. As an example, in onion I, interplanar distances between first and second shells ($d = 0.37$ nm) and between third and fourth shells ($d = 0.31$ nm) deviate by 10% from that of the interplanar distance in bulk BN ($d_{002} = 0.335$ nm).

Finally, it should be said that the formation of onions under an intense electron beam does not occur easily since it is very sensitive to different factors such as the crystallographic orientation of the BN sample with respect to the electron beam and the conditions of illumination.

2.2 BN *nanotubes powder irradiation experiments*

We now describe results from irradiation experiments of BN nanotubes in a Jeol 4000FX. A typical evolution of a tube having a reduced number of layers is shown in Fig. 2. First the outer layers undulate and are cut locally into small segments which bend and close to form cages irregular in shape (Fig. 2a,b). These cages of initial diameter in the range of 1–2 nm are then broken up into smaller cages which agglomerate as soap bubbles (Fig. 2c,d). The smallest diameters are approximately 0.4 nm. It is likely that the bubbles are attracted by van der Waals forces, and build close-packed arrangements. Once formed, the small bubbles are very volatile

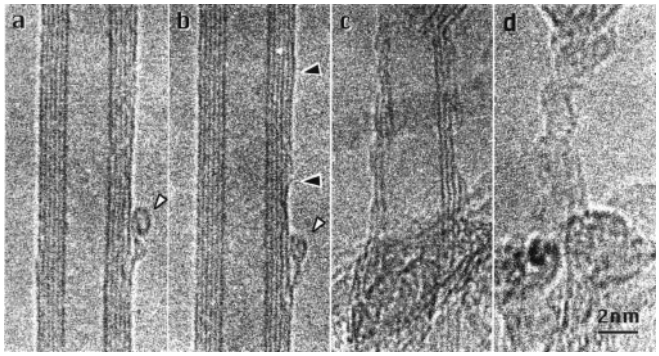

Fig. 2a–d. Temporal sequence of high-resolution images of a six-layer BN nanotube subjected to an intense electron beam. Irradiation times were a few minutes in **a** and **b**, 20 min in **c**, and 40 min in **d**. Strong irradiation was stopped a few minutes before taking micrographs. The *white arrows* indicate a cage breaking into small pieces whereas *black arrows* indicate undulating parts of the outer layer

and disappear rapidly. The very faint contrast of Fig. 2d (with respect to Fig. 2a) accounts for an important loss of atoms. In such a process, the nanotube appears to be peeled off until the internal layer is broken and disappears. Figure 3 shows an irradiation sequence of a nanotube with more layers. In that case, irradiation simultaneously affects outer and inner layers. When outer layers undulate and break as previously described, inner layers separate from their neighboring layer (as clearly seen in Fig. 3b,c), shrink, and break into small pieces which close to form bubbles as small as 0.5–1 nm in diameter. An example of a shrunk inner layer breaking into two small cages is emphasized in the inset of Fig. 3b. The final state is the same as for narrower tubes (Fig. 3d).

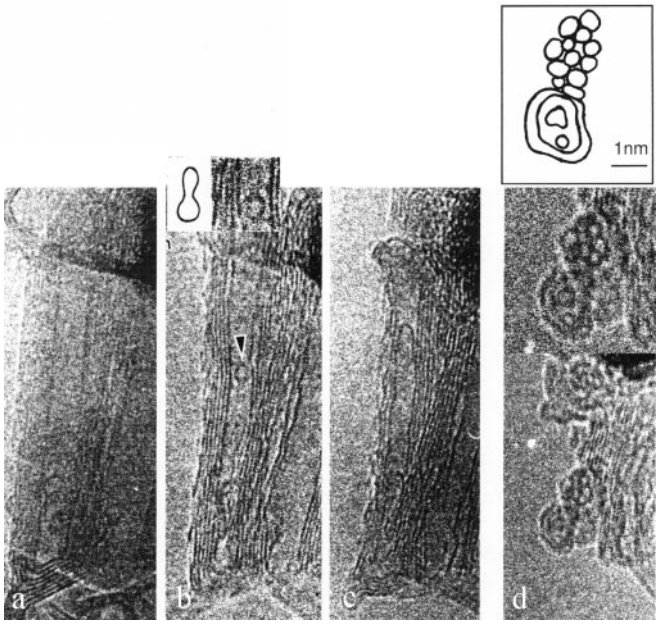

Fig. 3a–d. Temporal sequence of a set of nanotubes having different numbers of layers under intense electron beam irradiation as in Fig. 2. **a** Initial state. Irradiation times were 10 min in **b**, 20 min in **c**, and 40 min in **d**. Note that nanotubes with two or three layers transform more rapidly than ten-layer tubes. Insets in **b** and **d** are magnifications of the arrowed objects. Details to be seen in these insets have been traced off and redrawn for clarity

The inset of Fig. 3d emphasizes the structure of the nanotube in the last stage of the process: one portion of the tube is already entirely transformed in a close packing of small bubbles whereas for the other portion, the transformation of the layers is not completely achieved. It is worth mentioning that two- or three-layer tubes are entirely transformed within approximately 10 min whereas 40-min irradiation is needed to achieve the transformation of ten-layer tubes. These times are to be compared to the times necessary to grow onions from carbon nanotubes which were typically 10 min with the present microscope.

Finally it is worth noting that in contrast to the onion formation from bulk BN samples, the transformation process of BN nanotubes into agglomerates of small cages is very easily observed. This may be due the fact that for nanotubes the basal layers are already curved which facilitates their bending under an intense beam.

3 Discussion

As for carbon, under strong electron irradiation, BN layers have a natural tendency towards bending and forming curled shells. However, in contrast to carbon, the irradiation derivatives display different morphologies depending on the starting materials and on the irradiation conditions: close-packed small cage-like molecules weakly interacting by van der Waals forces or small concentric nested polyhedral cages. Another difference in the formation process – compared to carbon – is that a significant loss of matter is observed here in both cases. For the onion formation, this loss of matter is not observed in [24] for the carbon system, whereas it can be clearly seen in Fig. 1 from the fact that the transformation towards the final configuration occurs at a constant number of shells, while the diameters of the shells decrease. By relying on observations from Fig. 1d, we speculate that the growth mechanism is an innermost-shell-driven process, where first the internal shells reach their stable configuration by means of atom ejection towards peripheral layers. The atomic flux towards the surface is compensated by the desorbtion of atoms in excess in the very external shell. This loss of matter – due to vaporization or sputtering of atoms – is also clearly observed during BN-nanotube irradiation experiments as shown in Fig. 2 where a six-layer nanotube is shown to reduce in diameter as its number of layers decreases.

A remarkable feature of the images shown in Fig. 1 is the polygonal shape with a small number of sides (typically 4 to 6) of the fringe patterns, which contrasts with the carbon onion images which are either quasi-circular or polygonal with typically 10 sides [25]. Besides, the diameter of the smallest shells is found to be significantly smaller than that of C_{60}, the most commonly observed smallest carbon cage. In order to interpret the observed morphology one has to look into the problem of the closure on itself of a BN hexagonal network. Because of the chemical bonding requirement that B and N atoms prefer to alternate, it has been suggested that BN analogs to carbon fullerenes are formed from combinations of odd member rings, i.e. cyclic B_2N_2 and B_3N_3 [12, 13]. According to Euler's theorem, six squares (instead of 12 pentagons in carbon fullerenes) are needed to close the structure. By following the geometrical construction scheme already used to construct carbon fullerenes with icosahedral symme-

try [26, 27] it was shown that an infinite family of cages with octahedral symmetry composed of alternating BN units can be built [21]. The eight equilateral triangular faces of the octahedron are cut from the hexagonal network and the six apexes are truncated by squares. The smallest cages observed in the final stage of our irradiation experiments, namely the onion internal shells or the individual cages packed in agglomerates, have a diameter of typically 0.4–0.7 nm. This range of diameters is comparable to that of the $B_{12}N_{12}$, $B_{16}N_{16}$, and $B_{28}N_{28}$ polyhedra, which were proposed theoretically as the smallest high-symmetry octahedral clusters with particularly high stability [13, 14]. We note that the $B_{12}N_{12}$ cluster is the smallest BN cage that can be composed of squares separated by hexagons, and was therefore suggested to be the analog to C_{60} [13].

As for their carbon analogs, an onion structure can then be built as a Russian doll assembly of cages increasing in size with an intercage distance close to that of bulk h-BN, namely $d = 0.335$ nm. Starting from a $B_{12}N_{12}$ cluster, the construction of a five-shell onion ($B_{12}N_{12}$; 5) results in the following nesting: $B_{12}N_{12}@B_{76}N_{76}@B_{208}N_{208}@B_{412}N_{412}@B_{676}N_{676}$. The intercage distances deviate from the ideal bulk value of 0.335 nm by less than 0.015 nm. Figure 4 shows a representation of this series of octahedral BN cages after structural relaxation by atomistic calculations. Note that in this particular series there is no orientational order between layers, which are packed in a turbostratic fashion. In the case of carbon, the icosahedral series $C_{60}@C_{240}@C_{540}@\ldots@C_{60n^2}$, often used to simulate carbon onions [25, 28, 29], leads to an intercage distance remarkably close to that of bulk graphite and has a perfect orientational order of the layers in the radial direction. The orientationally ordered series starting from $B_{12}N_{12}$, namely $B_{12}N_{12}@B_{48}N_{48}@\ldots@B_{12n^2}N_{12n^2}$, is not realistic because the intercage distance is much too small ($d = 0.2$ nm). If the orientation between layers was to be favorable, either in the stability of the structure or in the growth process, the orientationally ordered BN onion with the intercage distance closest to 0.335 nm would be $B_{36}N_{36}@B_{144}N_{144}@\ldots@B_{36n^2}N_{36n^2}$ with $d \approx 0.346$ nm. The innermost shells have a tendency to shrink, possibly down to $B_{12}N_{12}$. For the larger shells, there is a competition between the tendency to follow this shrinking process in order to preserve the intercage distance, and the inertia to do so while preserving the orientation of the layers. This could explain the large deviations from the expected value mentioned above in the intercage in onion I between inner shells.

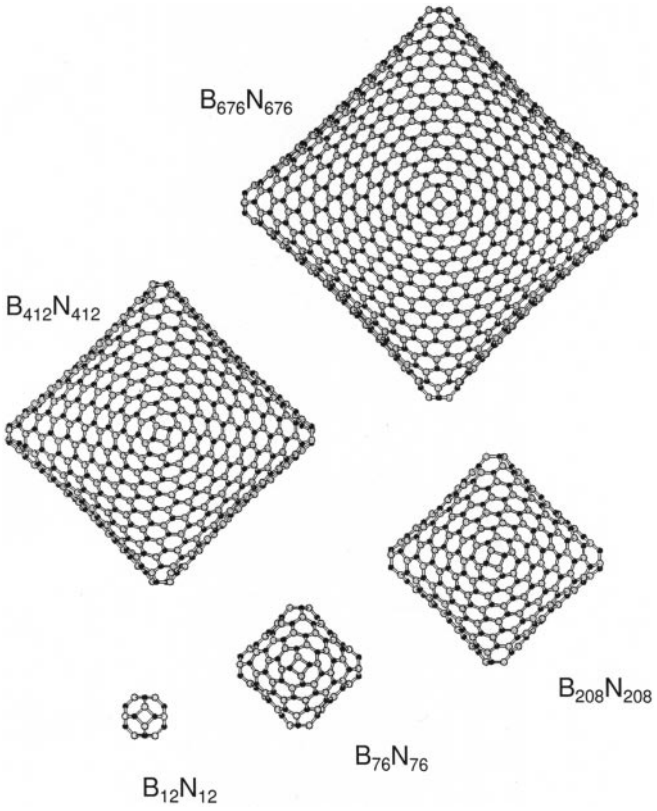

Fig. 4. Series of octahedral cages building a 5-layer onion: $B_{12}N_{12}$, $B_{76}N_{76}$, $B_{208}N_{208}$, $B_{412}N_{412}$, $B_{676}N_{676}$ after structural relaxation by atomistic calculations

In order to have more insight into the 3-D geometry of the observed nested cages, the HREM experimental images were compared with simulated images of the ideal structure constructed above [30]. In agreement with the experiment, polygonal shapes with either four or six sides are obtained, depending on the orientation of the electron beam. A set of four images corresponding to four particular high-symmetry orientations is displayed in Fig. 5. The observed shape is either square-like, hexagonal-like, or rather elongated with a strong contrast displaying a 2-fold axis symmetry. All three types of geometry are experimentally observed as the onions evolve towards a stable configuration and rotate, setting therefore successive crystallographic orientations along the viewing direction. Since the onions are supported on a flat surface, the most stable configuration is obtained when they are lying on one of their triangular faces. As a consequence, the most probable shape of their 2-D-image is the square-like shape. A distorted hexagonal shape is seen for onion I in Fig. 1e. An elongated shape with a strong 2-fold axis symmetry is detected for onion II in Fig. 1f. The square-like shape is observed for onions I and II in Figs. 1g and 1h, respectively. From the respective side length of the observed innermost squares, we suggest that the innermost cages of onions I and II in Figs. 1g and 1h are respectively close to a $B_{12}N_{12}$ molecule and a $B_{16}N_{16}$ molecule.

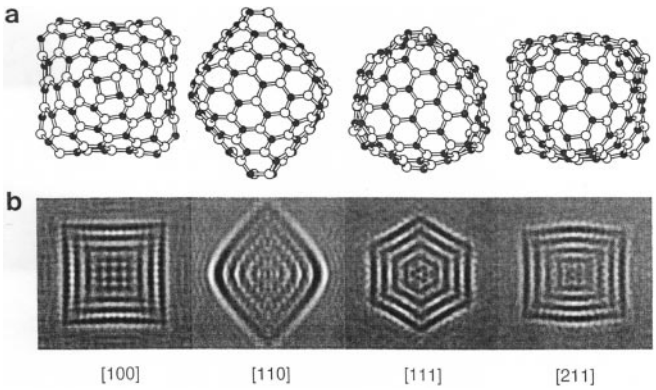

Fig. 5a,b. In **a** 3-D representation of the $B_{76}N_{76}$ molecule viewed in [100], [110], [111], and [211] directions. The three basis vectors are defined as joining the center of the octahedron and three adjacent apexes respectively. In **b** simulated images of a ($B_{12}N_{12}$; 5) onion viewed in the corresponding directions. The simulations are performed for the characteristics of the Jeol 3000F microscope used in the present experiments, and are shown here for a defocus of 60 nm

As a final point, we want to discuss the shape of the peripheral onion layers. Although for internal shells, the simulated images are in good agreement with the proposed octahedral symmetry structure, important deviations are observed for larger cages (outer shells of the onions) which are more rounded in shape. Such deviation from the predicted structure was also observed for large carbon onions whose perfect spherical geometry is in disagreement with a perfect icosahedral symmetry. A first model was proposed suggesting that the observed sphericity is caused by a random orientation of the icosahedral concentric shells (loss of the epitaxial arrangement of pentagons), attenuating the sharp aspect of the apexes where the pentagons are located [29]. By following this idea, the misorientation of the octahedral concentric shells observed in onion II (Fig. 1h) could be responsible for the deformation of the planar sectors and therefore for the rounded shape of the largest cages. However, such misorientation effect cannot account for the rounded shape of the apexes in onion I since the square rings are epitaxially stacked (Fig. 1g). A complementary explanation was proposed for carbon onions: the incorporation of pairs of 5- and 7-member rings was shown to transform the initially strongly faceted icosahedral structure into a more spherical shape [31, 32]. The formation of such defects is indeed expected under intense irradiation. Moreover, it was shown that these defects can also be thermally generated at high temperatures [32]. A local increase of the temperature can also be induced by irradiation. The direct transposition to the case of BN is obtained by incorporating pairs of 4- and 8-member rings, if chemical frustrations are not allowed. However, the insertion of pairs of 4-member and 8-member rings introduces important structural stress. Despite local chemical frustration induced by the introduction of even-member rings in a BN network, incorporation of pairs of 5- and 7-member rings has to be envisaged for large BN cages to build a low-stress structure.

4 Conclusions

Intense electron irradiation experiments were carried on two kinds of BN samples, a BN-nanotube powder and a novel turbostratic BN material. As for carbon and for BN powders, irradiation provokes a tendency towards curling and forming shells. However in contrast to carbon, both materials display different specific behaviors which lead either to the formation of agglomerates of small cage-like molecules weakly packed by van der Waals forces or to that of small nested polyhedral cages. The overall shape of the BN cages was explained within the frame of the octahedral model previously proposed for BN analogs to carbon fullerenes. As for carbon, the observed structure is more spherical in shape than the ideal polyhedral structure. The difference can be explained by the insertion of pairs of defects. Whatever the starting materials, under electron radiation unstable large cages transform into smaller shells until the individual cages or the innermost shell of the onions is 0.4–0.7 nm in diameter. This range in diameter corresponds to that of the octahedral polyhedra $B_{12}N_{12}$, $B_{16}N_{16}$, and $B_{28}N_{28}$, which were predicted to be magic BN clusters from electronic structure calculations [14]. Although their formation mechanism remains to be understood, the present study brings the first experimental evidence for the existence of small BN cages analogous to carbon fullerenes.

Acknowledgements. We are grateful to H. Pascard and N. Demoncy for providing us with the BN nanotube sample. Part of this work was supported by the Center Of Excellence Project at the National Institute for Research in Inorganic Materials, Tsukuba, Japan.

References

1. H.W. Kroto, J.R. Health, S.C. O'Brien, R.F. Curl, R.E. Smalley: Nature **318**, 162 (1985)
2. S. Iijima: Nature **354**, 56 (1991)
3. N.G. Chopra, R.J. Luyken, K. Cherrey, V.H. Crespi, M.L. Cohen, S.G. Louie, A. Zettl: Science **269**, 966 (1995)
4. D. Goldberg, Y. Bando, M. Eremets, K. Takemura, K. Kurashima, H. Yusa: Appl. Phys. Lett. **69**, 2045 (1996)
5. A. Loiseau, F. Willaime, N. Demoncy, G. Hug, H. Pascard: Phys. Rev. Lett. **76**, 4737 (1996)
6. M. Terrones, W.K. Hsu, H. Terrones, J.P. Zhang, S. Ramos, J.P. Hare, R. Castillo, K. Prassides, A.K. Cheetham, H.W. Kroto, D.R.M. Walton: Chem. Phys. Lett. **259**, 568 (1996)
7. O. Stéphan, P.M. Ajayan, C. Colliex, Ph. Redlich, J.M. Lambert, P. Bernier, P. Lefin: Science **266**, 1683 (1994)
8. Z. Weng-Zieh, K. Cherrey, N.G. Chopra, X. Blase, Y. Miyamoto, A. Rubio, M.L. Cohen, S.G. Louie, A. Zettl, R. Gronsky: Phys. Rev. B **51**, 11229 (1995)
9. R. Tenne, L. Margulis, M. Genut, G. Hodes: Nature **360**, 444 (1992)
10. L. Boulanger, F. Willaime, M. Cauchetier: In ICEM 13 Proceedings, ed. by B. Jouffrey, C. Colliex, Vol. III. A (Les Editions de Physique, Paris 1994) p. 315
11. L. Boulanger, B. Andriot, M. Cauchetier, F. Willaime: Chem. Phys. Lett. **234**, 227 (1995)
12. J.R. Browser, D.A. Jelski, T.F. George: Inorg. Chem. **31**, 154 (1992)
13. F. Jensen, H. Toflund: Chem. Phys. Lett. **201**, 89 (1993)
14. G. Seifert, P.W. Fowler, D. Mitchell, D. Porezag, Th. Frauenheim: Chem. Phys. Lett. **268**, 352 (1997)
15. D. Ugarte: Nature **359**, 707 (1992); P.J.F. Harris, S.C. Tsang, J.B. Claridge, M.L.H. Green: J. Chem. Soc., Faraday Trans. **90**, 2799 (1994)
16. G. Lulli, A. Parisini, G. Mattei: Ultramicroscopy **60**, 187 (1995)
17. T. Fuller, F. Banhart: Chem. Phys. Lett. **254**, 372 (1996)
18. F. Banhart, M. Zwanger, H.J. Muhr: Chem. Phys. Lett. **231**, 98 (1994)
19. M. Jose-Yacaman, H. Lopez, P. Santiago, D.H. Galvan, J.L. Garzon, A. Reyes: Appl. Phys. Lett. **69**, 1065 (1996)
20. O. Stéphan, Y. Bando, C. Dussarrat, K. Kurashima, T. Sasaki, T. Tamiya, M. Akaishi: Appl. Phys. Lett. **70**, 2383 (1997)
21. H.-Y. Zhu, D.J. Klein, W.A. Seitz, N.H. March: Inorg. Chem. **34**, 1383 (1995)
22. T. Sato: In Research Report of NIRIM, Vol. 89, Chap. 3 (NIRIM, Tsukuba 1996), pp. 12–13
23. M. Hubacek, T. Sato: J. Solid State Chem. **114**, 258 (1995)
24. D. Ugarte: Chem. Phys. Lett. **207**, 473 (1993)
25. Q. Ru, M. Okamoto, Y. Kondo, K. Takayanagi: Chem. Phys. Lett. **259**, 425 (1996)
26. M. Goldberg: Tohoku Math. J. **43**, 104 (1937)
27. H.S.M. Coexeter: In *A Spectrum of Mathematics*, ed. by J.C. Butcher, (Auckland University Press, Auckland 1971)
28. D. Ugarte: Europhys. Lett. **22**, 45 (1993)
29. K.G. McKay, H. Kroto, D.J. Wales: J. Chem. Soc., Faraday Trans. **88**, 2815 (1992)
30. The simulated images were calculated by a multislice method, making use of the EMS software described in: P.A. Stadelman: Ultramicroscopy **21**, 131 (1987)
31. M. Terrones, H. Terrones: Fullerene Sci. Technol. **4**, 517 (1997)
32. C.J. Brabec, A. Maiti, J. Bernholc: Chem. Phys. Lett. **219**, 473 (1994)